SCIENCE CHINA
Physics, Mechanics & Astronomy

• Research Paper •

April 2010 Vol.53 No.4: 758–766
doi: 10.1007/s11433-010-0159-1

An interpolating boundary element-free method (IBEFM) for elasticity problems

REN HongPing[1], CHENG YuMin[2*] & ZHANG Wu[1]

[1] *School of Computer Engineering and Science, Shanghai University, Shanghai 200072, China;*
[2] *Shanghai Institute of Applied Mathematics and Mechanics, Shanghai University, Shanghai 200072, China*

Received November 2, 2009; accepted January 27, 2010

The paper begins by discussing the interpolating moving least-squares (IMLS) method. Then the formulae of the IMLS method obtained by Lancaster are revised. On the basis of the boundary element-free method (BEFM), combining the boundary integral equation method with the IMLS method improved in this paper, the interpolating boundary element-free method (IBEFM) for two-dimensional elasticity problems is presented, and the corresponding formulae of the IBEFM for two-dimensional elasticity problems are obtained. In the IMLS method in this paper, the shape function satisfies the property of Kronecker δ function, and then in the IBEFM the boundary conditions can be applied directly and easily. The IBEFM is a direct meshless boundary integral equation method in which the basic unknown quantity is the real solution to the nodal variables. Thus it gives a greater computational precision. Numerical examples are presented to demonstrate the method.

moving least-squares (MLS) approximation, interpolating moving least-squares (IMLS) method, boundary integral equation, meshless method, boundary element-free method (BEFM), interpolating boundary element-free method (IBEFM), elasticity problem

PACS: 02.60.Ed, 02.70.-c, 02.70.Pt, 46.15.-x

In recent years, more and more attention has been paid to research on the meshless (or meshfree) method [1,2]. The meshless method has some advantages over the traditional computational methods, such as finite element method (FEM) and boundary element method (BEM).

The meshless boundary integral equation method points to one of the important research directions of the meshless method. Combining different approximation functions in the meshless method with the boundary integral equation method, researchers have developed meshless boundary integral equation methods, such as the boundary node method (BNM) [3–5], the local boundary integral equation (LBIE) method [6–8], and the boundary element-free method (BEFM) [9–19].

The moving least-squares (MLS) approximation is one of the bases of the meshless method [1,2,20]. The meshless method based on the MLS approximation can generate a solution possessing great precision. The meshless boundary integral equation methods are developed by combining the MLS approximation with boundary integral equation methods [3–19]. The boundary node method (BNM) is one of the meshless boundary integral equation methods, and Mukherjee et al. [3–5] used it to solve potential problems and linear elasticity problems. Another equally important method of the meshless boundary integral equation methods is the local boundary integral equation (LBIE) method, which Atluri et al. [6–8] present to solve linear and nonlinear boundary value problems. In the BNM, the basic unknown quantities are approximations of the nodal variables. However, as they are not the real nodal variables, the boundary conditions cannot be directly applied. In the LBIE method, the traction term is not included in the local boundary integral equations.

*Corresponding author (email: ymcheng@shu.edu.cn)

The LBIE method can easily solve a problem with a complicated boundary, but the local foundational solution is more complicated than it is when the conventional boundary element method is used. Moreover, in the LBIE method, the basic unknown quantities are also approximations of the nodal variables, and, again, the boundary conditions cannot be applied directly. The BNM and the LBIE method both are the indirect meshless boundary integral equation methods.

The MLS approximation is developed from the conventional least-squares method, and in practical numerical processes, the MLS approximation is the conventional least-squares method for every selected point. A disadvantage of the conventional least-squares method is that the final algebra equations system is sometimes ill-conditioned or singular. Then Cheng and Liew et al. [9,10] improved the moving least-squares approximation. In the improved moving least-squares approximation, the algebra equation system is not ill-conditioned or singular, and the solution of the algebra equation system can be obtained directly without obtaining the inverse matrix. There are also fewer coefficients in the improved moving least-squares approximation than there are in the MLS approximation, and hence the computing speed and efficiency have increased. Combining the boundary integral equation method with the improved moving least-squares approximation, Cheng and Liew et al. [9–19] come up with a direct meshless boundary integral equation method, called boundary element-free method (BEFM), to solve the problems, such as potential problems, elasticity, elastodynamics, and fracture. And the improved element-free Galerkin method based on the improved moving least-squares approximation was discussed by Zhang, Liew and Cheng [21–23]. Cheng and Liew et al. [24–26] presented complex variable moving least-squares approximation.

In the BEFM, the basic unknown quantities are the real solutions to the nodal variables, but in the BNM and the LBIE method, the basic unknown quantities are approximations of the nodal variables. The BEFM as a direct meshless boundary integral equation method has a greater computational precision. In the BEFM, boundary conditions are applied directly. But in the improved moving least-squares approximation, the shape function does not satisfy the property of Kronecker δ function, and the boundary conditions are applied with constraints in the BEFM. This is a problem in the BEFM and must be solved from the perspective of mathematical theories. The interpolating moving least-squares (IMLS) method presented by Lancaster [20] can obtain the shape function which satisfies the property of Kronecker δ function. If we apply the IMLS method to the BEFM, the boundary conditions can be applied directly. In this paper, a new method to obtain the shape function of the MLS approximation is given, and then the IMLS method is discussed, and the formulae of the IMLS method obtained by Lancaster are revised. Then on the basis of the BEFM, and by combining the boundary integral equation method with the IMLS method, the paper presents the interpolating boundary element-free method (IBEFM) for two-dimensional elasticity problems, and the corresponding formulae of the IBEFM for two-dimensional elasticity problems. The IBEFM is a direct meshless boundary integral equation method in which the basic unknown quantity is the real solution to the nodal variables, and the boundary conditions can be applied directly and easily. Thus it gives a greater computational precision. Numerical examples are presented to demonstrate the method.

1 Moving least-squares approximation

In the MLS approximation, the trial function is

$$u^h(\boldsymbol{x}) = \sum_{i=1}^{m} p_i(\boldsymbol{x}) a_i(\boldsymbol{x}) = \boldsymbol{p}^{\mathrm{T}}(\boldsymbol{x})\boldsymbol{a}(\boldsymbol{x}), \tag{1}$$

where $p_i(\boldsymbol{x})$, $i = 1,2,\cdots,m$, are monomial basis functions, m is the number of terms in the basis, and $a_i(\boldsymbol{x})$ are the coefficients of the basis functions.

In general, the basis functions are as follows:
Linear basis:

$$\boldsymbol{p}^{\mathrm{T}} = (1, x_1), \quad \text{in 1D}, \tag{2}$$

$$\boldsymbol{p}^{\mathrm{T}} = (1, x_1, x_2), \quad \text{in 2D}. \tag{3}$$

Quadratic basis:

$$\boldsymbol{p}^{\mathrm{T}} = (1, x_1, x_1^2), \quad \text{in 1D}, \tag{4}$$

$$\boldsymbol{p}^{\mathrm{T}} = (1, x_1, x_2, x_1^2, x_1x_2, x_2^2), \quad \text{in 2D}. \tag{5}$$

The local approximation that is defined by Lancaster and Salkauskas [20] is

$$u^h(\boldsymbol{x}, \bar{\boldsymbol{x}}) = \sum_{i=1}^{m} p_i(\bar{\boldsymbol{x}}) a_i(\boldsymbol{x}) = \boldsymbol{p}^{\mathrm{T}}(\bar{\boldsymbol{x}})\boldsymbol{a}(\boldsymbol{x}). \tag{6}$$

For the precise local approximation of the function $u(\boldsymbol{x})$, the difference between the local approximation $u^h(\boldsymbol{x})$ and the function $u(\boldsymbol{x})$ must be minimized by a weighted least-squares method.

Define a functional

$$\begin{aligned} J &= \sum_{I=1}^{n} w(\boldsymbol{x} - \boldsymbol{x}_I)[u^h(\boldsymbol{x}, \boldsymbol{x}_I) - u(\boldsymbol{x}_I)]^2 \\ &= \sum_{I=1}^{n} w(\boldsymbol{x} - \boldsymbol{x}_I)\left[\sum_{i=1}^{m} p_i(\boldsymbol{x}_I)\cdot a_i(\boldsymbol{x}) - u(\boldsymbol{x}_I)\right]^2, \end{aligned} \tag{7}$$

where $w(\boldsymbol{x} - \boldsymbol{x}_I)$ is a weight function with compact support, and $\boldsymbol{x}_I$, $I = 1,2,\cdots,n$, are the nodes in the influence domain of point $\boldsymbol{x}$.

Eq. (7) is written as

$$J = (\boldsymbol{Pa} - \boldsymbol{u})^{\mathrm{T}} \boldsymbol{W}(\boldsymbol{x})(\boldsymbol{Pa} - \boldsymbol{u}), \tag{8}$$

where

$$\boldsymbol{u} = (u_1, u_2, \cdots, u_n)^{\mathrm{T}} = (u(\boldsymbol{x}_1), u(\boldsymbol{x}_2), \cdots, u(\boldsymbol{x}_n))^{\mathrm{T}}, \tag{9}$$

$$\boldsymbol{P} = \begin{bmatrix} p_1(\boldsymbol{x}_1) & p_2(\boldsymbol{x}_1) & \cdots & p_m(\boldsymbol{x}_1) \\ p_1(\boldsymbol{x}_2) & p_2(\boldsymbol{x}_2) & \cdots & p_m(\boldsymbol{x}_2) \\ \vdots & \vdots & \ddots & \vdots \\ p_1(\boldsymbol{x}_n) & p_2(\boldsymbol{x}_n) & \cdots & p_m(\boldsymbol{x}_n) \end{bmatrix} = (\boldsymbol{p}_1, \boldsymbol{p}_2, \cdots, \boldsymbol{p}_m), \tag{10}$$

$$\boldsymbol{W}(\boldsymbol{x}) = \begin{bmatrix} w(\boldsymbol{x} - \boldsymbol{x}_1) & 0 & \cdots & 0 \\ 0 & w(\boldsymbol{x} - \boldsymbol{x}_2) & \cdots & 0 \\ \vdots & \vdots & \ddots & \vdots \\ 0 & 0 & \cdots & w(\boldsymbol{x} - \boldsymbol{x}_n) \end{bmatrix}, \tag{11}$$

$$\boldsymbol{a} = \boldsymbol{a}(\boldsymbol{x}) = (a_1(\boldsymbol{x}), a_2(\boldsymbol{x}), \cdots, a_n(\boldsymbol{x}))^{\mathrm{T}}. \tag{12}$$

On the space $\mathrm{span}(\boldsymbol{p}_1, \boldsymbol{p}_2, \cdots, \boldsymbol{p}_m)$, the following inner product

$$(\boldsymbol{f}, \boldsymbol{g})_{\boldsymbol{x}} = \sum_{I=1}^{n} w(\boldsymbol{x} - \boldsymbol{x}_I) f(\boldsymbol{x}_I) g(\boldsymbol{x}_I) \tag{13}$$

is defined for $\forall \boldsymbol{f}(\boldsymbol{x})$, $\boldsymbol{g}(\boldsymbol{x}) \in \mathrm{span}(\boldsymbol{p}_1, \boldsymbol{p}_2, \cdots, \boldsymbol{p}_m)$. The norm of $\boldsymbol{f}(\boldsymbol{x})$ is defined as

$$\|\boldsymbol{f}\|_{\boldsymbol{x}} = [(\boldsymbol{f}, \boldsymbol{f})_{\boldsymbol{x}}]^{\frac{1}{2}}. \tag{14}$$

Here, a function with the subscript $\boldsymbol{x}$ represents the function related to the selected point $\boldsymbol{x}$ in $\boldsymbol{a}(\boldsymbol{x})$ and the weight function $w(\boldsymbol{x} - \boldsymbol{x}_I)$. The inner product (13) and the norm (14) are also taken as the inner product and the norm of the corresponding functions, respectively.

From eq. (8) we have

$$J = \|\boldsymbol{Pa} - \boldsymbol{u}\|_{\boldsymbol{x}}^2 = \|a_1 \boldsymbol{p}_1 + a_2 \boldsymbol{p}_2 + \cdots + a_m \boldsymbol{p}_m - \boldsymbol{u}\|_{\boldsymbol{x}}^2. \tag{15}$$

Then

$$J = \|\boldsymbol{u}^{(1)} - \boldsymbol{u}\|_{\boldsymbol{x}}^2 \tag{16}$$

is the minimum of the functional J, where $\boldsymbol{u}^{(1)}$ is the projection of $\boldsymbol{u}$ in $\mathrm{span}(\boldsymbol{p}_1, \boldsymbol{p}_2, \cdots, \boldsymbol{p}_m)$.

Let

$$\boldsymbol{u} = \boldsymbol{u}^{(1)} + \boldsymbol{u}^{(2)}, \tag{17}$$

where

$$\boldsymbol{u}^{(1)} \in \mathrm{span}(\boldsymbol{p}_1, \boldsymbol{p}_2, \cdots, \boldsymbol{p}_m), \tag{18}$$

$$\boldsymbol{u}^{(2)} \perp \mathrm{span}(\boldsymbol{p}_1, \boldsymbol{p}_2, \cdots, \boldsymbol{p}_m). \tag{19}$$

Then

$$(\boldsymbol{p}_i, \boldsymbol{u}^{(2)})_{\boldsymbol{x}} = 0, \quad (i = 1, 2, \cdots, m). \tag{20}$$

From eq. (17), we have

$$(\boldsymbol{p}_i, \boldsymbol{u})_{\boldsymbol{x}} = (\boldsymbol{p}_i, \boldsymbol{u}^{(1)})_{\boldsymbol{x}} + (\boldsymbol{p}_i, \boldsymbol{u}^{(2)})_{\boldsymbol{x}} = (\boldsymbol{p}_i, \boldsymbol{u}^{(1)})_{\boldsymbol{x}}, \quad (i = 1, 2, \cdots, m), \tag{21}$$

i.e.

$$(\boldsymbol{p}_i, \boldsymbol{u})_{\boldsymbol{x}} = (\boldsymbol{p}_i, \boldsymbol{u}^{(1)})_{\boldsymbol{x}} = (\boldsymbol{p}_i, \sum_{j=1}^{m} a_j(\boldsymbol{x}) \boldsymbol{p}_j)_{\boldsymbol{x}}, \quad (i = 1, 2, \cdots, m). \tag{22}$$

Eq. (22) is written as

$$\begin{bmatrix} (\boldsymbol{p}_1, \boldsymbol{p}_1)_{\boldsymbol{x}} & (\boldsymbol{p}_1, \boldsymbol{p}_2)_{\boldsymbol{x}} & \cdots & (\boldsymbol{p}_1, \boldsymbol{p}_m)_{\boldsymbol{x}} \\ (\boldsymbol{p}_2, \boldsymbol{p}_1)_{\boldsymbol{x}} & (\boldsymbol{p}_2, \boldsymbol{p}_2)_{\boldsymbol{x}} & \cdots & (\boldsymbol{p}_2, \boldsymbol{p}_m)_{\boldsymbol{x}} \\ \vdots & \vdots & \ddots & \vdots \\ (\boldsymbol{p}_m, \boldsymbol{p}_1)_{\boldsymbol{x}} & (\boldsymbol{p}_m, \boldsymbol{p}_2)_{\boldsymbol{x}} & \cdots & (\boldsymbol{p}_m, \boldsymbol{p}_m)_{\boldsymbol{x}} \end{bmatrix} \begin{bmatrix} a_1(\boldsymbol{x}) \\ a_2(\boldsymbol{x}) \\ \vdots \\ a_m(\boldsymbol{x}) \end{bmatrix} = \begin{bmatrix} (\boldsymbol{p}_1, \boldsymbol{u})_{\boldsymbol{x}} \\ (\boldsymbol{p}_2, \boldsymbol{u})_{\boldsymbol{x}} \\ \vdots \\ (\boldsymbol{p}_m, \boldsymbol{u})_{\boldsymbol{x}} \end{bmatrix}, \tag{23}$$

i.e.

$$\boldsymbol{A}(\boldsymbol{x})\boldsymbol{a}(\boldsymbol{x}) = \boldsymbol{B}(\boldsymbol{x})\boldsymbol{u}, \tag{24}$$

where matrices $\boldsymbol{A}(\boldsymbol{x})$ and $\boldsymbol{B}(\boldsymbol{x})$ are

$$\boldsymbol{A}(\boldsymbol{x}) = \boldsymbol{P}^{\mathrm{T}} \boldsymbol{W}(\boldsymbol{x}) \boldsymbol{P}, \tag{25}$$

$$\boldsymbol{B}(\boldsymbol{x}) = \boldsymbol{P}^{\mathrm{T}} \boldsymbol{W}(\boldsymbol{x}). \tag{26}$$

From eq. (24) we obtain

$$\boldsymbol{a}(\boldsymbol{x}) = \boldsymbol{A}^{-1}(\boldsymbol{x}) \boldsymbol{B}(\boldsymbol{x}) \boldsymbol{u}. \tag{27}$$

The expression of the local approximation $u^h(\boldsymbol{x})$ is then

$$u^h(\boldsymbol{x}) = \boldsymbol{\varphi}(\boldsymbol{x}) \boldsymbol{u} = \sum_{I=1}^{n} \varphi_I(\boldsymbol{x}) u_I, \tag{28}$$

where $\boldsymbol{\varphi}(\boldsymbol{x})$ is called the shape function and

$$\boldsymbol{\varphi}(\boldsymbol{x}) = (\varphi_1(\boldsymbol{x}), \varphi_2(\boldsymbol{x}), \cdots, \varphi_n(\boldsymbol{x})) = \boldsymbol{p}^{\mathrm{T}}(\boldsymbol{x}) \boldsymbol{A}^{-1}(\boldsymbol{x}) \boldsymbol{B}(\boldsymbol{x}). \tag{29}$$

When $m = 1$, the approximation function is

$$u^h(\boldsymbol{x}) = \frac{\sum_{I=1}^{n} w(\boldsymbol{x} - \boldsymbol{x}_I) u_I}{\sum_{I=1}^{n} w(\boldsymbol{x} - \boldsymbol{x}_I)}. \tag{30}$$

2 The interpolating moving least-squares method

At the point $\boldsymbol{x}$, normalizing the basis function $p_1(\boldsymbol{x}) \equiv 1$, we have

$$\beta_{\boldsymbol{x}}^{(1)} = \frac{p_1}{\|p_1\|_{\boldsymbol{x}}} = \frac{1}{\left[\sum_{I=1}^{n} w(\boldsymbol{x}-\boldsymbol{x}_I)\right]^{\frac{1}{2}}}. \tag{31}$$

For $i = 2,3,\cdots,m,$ we can generate functions orthogonal to $\beta_{\boldsymbol{x}}^{(1)}$ as follows:

$$\begin{aligned} b_{\boldsymbol{x}}^{(i)}(\boldsymbol{x}) &= p_i(\boldsymbol{x}) - (p_i, \beta_{\boldsymbol{x}}^{(1)})_{\boldsymbol{x}} \beta_{\boldsymbol{x}}^{(1)} \\ &= p_i(\boldsymbol{x}) - \frac{\sum_{I=1}^{n} p_i(\boldsymbol{x}_I) w(\boldsymbol{x}-\boldsymbol{x}_I)}{\sum_{I=1}^{n} w(\boldsymbol{x}-\boldsymbol{x}_I)}, \end{aligned} \tag{32}$$

i.e.

$$b_{\boldsymbol{x}}^{(i)}(\boldsymbol{x}) = p_i(\boldsymbol{x}) - \sum_{I=1}^{n} p_i(\boldsymbol{x}_I) v(\boldsymbol{x}-\boldsymbol{x}_I), \tag{33}$$

where

$$v(\boldsymbol{x}-\boldsymbol{x}_I) = \frac{w(\boldsymbol{x}-\boldsymbol{x}_I)}{\sum_{I=1}^{n} w(\boldsymbol{x}-\boldsymbol{x}_I)}. \tag{34}$$

In the MLS, when the new basis functions $\beta_{\boldsymbol{x}}^{(1)}(\boldsymbol{x})$, $b_{\boldsymbol{x}}^{(2)}(\boldsymbol{x}), b_{\boldsymbol{x}}^{(3)}(\boldsymbol{x}), \cdots, b_{\boldsymbol{x}}^{(m)}(\boldsymbol{x})$ are used, the corresponding approximation function is

$$u^h(\boldsymbol{x}) = (u, \beta_{\boldsymbol{x}}^{(1)}(\boldsymbol{x}))_{\boldsymbol{x}} \beta_{\boldsymbol{x}}^{(1)}(\boldsymbol{x}) + \sum_{i=2}^{m} a_{i-1}(\boldsymbol{x}) b_{\boldsymbol{x}}^{(i)}(\boldsymbol{x}), \tag{35}$$

i.e.

$$u^h(\boldsymbol{x}) = \boldsymbol{v}^{\mathrm{T}}(\boldsymbol{x})\boldsymbol{u} + \boldsymbol{b}^{\mathrm{T}}(\boldsymbol{x})\boldsymbol{a}(\boldsymbol{x}), \tag{36}$$

where

$$\boldsymbol{v}(\boldsymbol{x}) = (v(\boldsymbol{x}-\boldsymbol{x}_1), v(\boldsymbol{x}-\boldsymbol{x}_2), \cdots, v(\boldsymbol{x}-\boldsymbol{x}_n))^{\mathrm{T}}, \tag{37}$$

$$\boldsymbol{b}(\boldsymbol{x}) = (b_{\boldsymbol{x}}^{(2)}(\boldsymbol{x}), b_{\boldsymbol{x}}^{(3)}(\boldsymbol{x}), \cdots, b_{\boldsymbol{x}}^{(m)}(\boldsymbol{x}))^{\mathrm{T}}, \tag{38}$$

$$\boldsymbol{a}(\boldsymbol{x}) = (a_1(\boldsymbol{x}), a_2(\boldsymbol{x}), \cdots, a_{m-1}(\boldsymbol{x}))^{\mathrm{T}}. \tag{39}$$

Then using the MLS approximation, we have

$$\boldsymbol{a}(\boldsymbol{x}) = \boldsymbol{A}_{\boldsymbol{x}}^{-1}(\boldsymbol{x})\boldsymbol{B}_{\boldsymbol{x}}(\boldsymbol{x})\boldsymbol{u}, \tag{40}$$

where

$$\boldsymbol{A}_{\boldsymbol{x}}(\boldsymbol{x}) = \boldsymbol{C}_{\boldsymbol{x}}^{\mathrm{T}} \boldsymbol{W}(\boldsymbol{x}) \boldsymbol{C}_{\boldsymbol{x}}, \tag{41}$$

$$\boldsymbol{B}_{\boldsymbol{x}}(\boldsymbol{x}) = \boldsymbol{C}_{\boldsymbol{x}}^{\mathrm{T}} \boldsymbol{W}(\boldsymbol{x}), \tag{42}$$

$$\boldsymbol{C}_{\boldsymbol{x}} = \begin{bmatrix} b_{\boldsymbol{x}}^{(2)}(\boldsymbol{x}_1) & b_{\boldsymbol{x}}^{(3)}(\boldsymbol{x}_1) & \cdots & b_{\boldsymbol{x}}^{(m)}(\boldsymbol{x}_1) \\ b_{\boldsymbol{x}}^{(2)}(\boldsymbol{x}_2) & b_{\boldsymbol{x}}^{(3)}(\boldsymbol{x}_2) & \cdots & b_{\boldsymbol{x}}^{(m)}(\boldsymbol{x}_2) \\ \vdots & \vdots & \ddots & \vdots \\ b_{\boldsymbol{x}}^{(2)}(\boldsymbol{x}_n) & b_{\boldsymbol{x}}^{(3)}(\boldsymbol{x}_n) & \cdots & b_{\boldsymbol{x}}^{(m)}(\boldsymbol{x}_n) \end{bmatrix}. \tag{43}$$

Substituting eq. (40) into eq. (36), we have

$$u^h(\boldsymbol{x}) = \boldsymbol{v}^{\mathrm{T}}(\boldsymbol{x})\boldsymbol{u} + \boldsymbol{b}^{\mathrm{T}}(\boldsymbol{x})\boldsymbol{A}_{\boldsymbol{x}}^{-1}(\boldsymbol{x})\boldsymbol{B}_{\boldsymbol{x}}(\boldsymbol{x})\boldsymbol{u}. \tag{44}$$

Eq. (44) is written as

$$u^h(\boldsymbol{x}) = \boldsymbol{\varphi}(\boldsymbol{x})\boldsymbol{u}, \tag{45}$$

where

$$\begin{aligned} \boldsymbol{\varphi}(\boldsymbol{x}) &= (\varphi_1(\boldsymbol{x}), \varphi_2(\boldsymbol{x}), \cdots, \varphi_n(\boldsymbol{x})) \\ &= \boldsymbol{v}^{\mathrm{T}}(\boldsymbol{x}) + \boldsymbol{b}^{\mathrm{T}}(\boldsymbol{x})\boldsymbol{A}_{\boldsymbol{x}}^{-1}(\boldsymbol{x})\boldsymbol{B}_{\boldsymbol{x}}(\boldsymbol{x}). \end{aligned} \tag{46}$$

When the weight function $w(\boldsymbol{x}-\boldsymbol{x}_I)$ is defined as

$$w(\boldsymbol{x}-\boldsymbol{x}_I) = \left|\boldsymbol{x}-\boldsymbol{x}_I\right|^{-\alpha}, \tag{47}$$

where α is an even positive integer, the function $u^{\mathrm{h}}(\boldsymbol{x})$ in eq. (45) can interpolate at all points $\{\boldsymbol{x}_I\}_{I=1}^{n}$, i.e.

$$u^h(\boldsymbol{x}_I) = u(\boldsymbol{x}_I). \tag{48}$$

Then we have

$$\varphi_I(\boldsymbol{x}_J) = \begin{cases} 1, & I = J, \\ 0, & I \neq J. \end{cases} \tag{49}$$

Corresponding to eq. (40), ref. [20] induces the following equation

$$\boldsymbol{a}(\boldsymbol{x}) = \boldsymbol{A}_{\boldsymbol{x}}^{-1}(\boldsymbol{x})\boldsymbol{B}_{\boldsymbol{x}}(\boldsymbol{x})(\boldsymbol{u} - (\boldsymbol{v}^{\mathrm{T}}(\boldsymbol{x})\boldsymbol{u})\boldsymbol{p}_1), \tag{50}$$

where $p_1(\boldsymbol{x}_I) = 1$. Then eq. (40) is different from eq. (50).

Since eq. (44) is different from the corresponding equation in ref. [20], the revised formulae of the IMLS approximation are given in this paper.

3 The interpolating boundary element-free method for two-dimensional elasticity

We consider the following two-dimensional problem in linear elasticity on the domain Ω bounded by the boundary Γ:

$$\sigma_{ji,j} + f_i = 0, \quad \boldsymbol{x} \in \Omega, \tag{51}$$

where σ_{ij} is the stress tensor and f_i is the body force.

The corresponding boundary conditions are given as follows:

$$u_i(\boldsymbol{x}) = \overline{u}_i(\boldsymbol{x}), \quad \boldsymbol{x} \in \Gamma_u, \tag{52}$$

$$t_i(\boldsymbol{x}) = \sigma_{ij}(\boldsymbol{x}) n_j = \overline{t}_i(\boldsymbol{x}), \quad \boldsymbol{x} \in \Gamma_\sigma, \tag{53}$$

where u_i are the displacements, t_i are the tractions, $\overline{u}_i$ and $\overline{t}_i$ are the prescribed displacements and tractions on the displacement boundary Γ_u and on the traction boundary Γ_σ, respectively, and n_i is the unit outward normal to the boundary Γ.

From the weighted residuals method, we obtain the following boundary integral equation [27]:

$$\begin{aligned} u_i(\xi) = &\int_\Gamma u_{ji}^*(\xi, \boldsymbol{x}) t_j(\boldsymbol{x}) \mathrm{d}\Gamma \\ &- \int_\Gamma t_{ij}^*(\xi, \boldsymbol{x}) u_j(\boldsymbol{x}) \mathrm{d}\Gamma \\ &+ \int_\Omega u_{ij}^*(\xi, \boldsymbol{x}) f_j(\boldsymbol{x}) \mathrm{d}\Omega, \end{aligned} \tag{54}$$

for the load point ξ that is located inside Ω, and

$$\begin{aligned} C_{ij}(\xi) u_j(\xi) = &\int_\Gamma u_{ij}^*(\xi, \boldsymbol{x}) t_j(\boldsymbol{x}) \mathrm{d}\Gamma \\ &- \int_\Gamma t_{ij}^*(\xi, \boldsymbol{x}) u_j(\boldsymbol{x}) \mathrm{d}\Gamma \\ &+ \int_\Omega u_{ij}^*(\xi, \boldsymbol{x}) f_j(\boldsymbol{x}) \mathrm{d}\Omega, \end{aligned} \tag{55}$$

for the load point ξ that is located on the boundary Γ. Here, C_{ki} is the function of the internal angle that the boundary Γ makes at the given point ξ; u_{ij}^* and t_{ij}^* chosen as the displacement and the traction of Kelvin's solution, are the *j*th components of the displacement and traction due to a unit load in the x_i direction.

For the convenience of discussion, we assume that the body force is zero.

The boundary Γ is separated into sub-domains Γ_n, $n = 1, 2, \cdots, N$. Here, N is the total number of the sub-domains. Then

$$\Gamma = \bigcup_{n=1}^{N} \Gamma_n, \tag{56}$$

and Γ_n and Γ_{n-1} are connected with a point. Γ_n is not a boundary element, so no shape function is dependent on it. Γ_n are used under the condition that the integrals in eqs. (55) and (54) are obtained numerically.

Eq. (55) is written as

$$\begin{aligned} C_{ki}(\xi) u_i(\xi) = &\sum_{n=1}^{N} \int_{\Gamma_n} u_{ki}^*(\xi, \boldsymbol{x}) t_i(\boldsymbol{x}) \mathrm{d}\Gamma \\ &- \sum_{n=1}^{N} \int_{\Gamma_n} t_{ki}^*(\xi, \boldsymbol{x}) u_i(\boldsymbol{x}) \mathrm{d}\Gamma, \end{aligned} \tag{57}$$

Some nodes are selected on each sub-domain Γ_n. The corresponding domain of influence for each node is built. The domains of influence of all the nodes must cover the boundary Γ.

From the expression of the approximation function (45), we let

$$u_i(\boldsymbol{x}) = \sum_{I=1}^{n_I} \varphi_I(\boldsymbol{x}) u_i(\boldsymbol{x}_I), \tag{58}$$

$$t_i(\boldsymbol{x}) = \sum_{I=1}^{n_I} \varphi_I(\boldsymbol{x}) t_i(\boldsymbol{x}_I). \tag{59}$$

Then eq. (57) becomes

$$\begin{aligned} C_{ki}(\xi_J) u_i(\xi_J) = &\sum_{n=1}^{N} \int_{\Gamma_n} u_{ki}^*(\xi_J, \boldsymbol{x}) \sum_{I=1}^{n_I} \varphi_I(\boldsymbol{x}) t_i(\xi_I) \mathrm{d}\Gamma \\ &- \sum_{n=1}^{N} \int_{\Gamma_n} t_{ki}^*(\xi_J, \boldsymbol{x}) \sum_{I=1}^{n_I} \varphi_I(\boldsymbol{x}) u_i(\xi_I) \mathrm{d}\Gamma, \end{aligned} \tag{60}$$

where ξ_I are nodes and n_I is the number of nodes with domains of influence that cover the field point $\boldsymbol{x}$.

Using the numerical method for the integrals in eq. (60), we have the following linear algebra equation:

$$\boldsymbol{C}^J \boldsymbol{U}^J + \boldsymbol{H}^J \boldsymbol{U} = \boldsymbol{G}^J \boldsymbol{T}, \tag{61}$$

where

$$\boldsymbol{U}^J = (u_{J1}, u_{J2})^{\mathrm{T}}, \tag{62}$$

$$\boldsymbol{U} = (u_{11}, u_{12}, u_{21}, u_{22}, \cdots, u_{n_I,1}, u_{n_I,2})^{\mathrm{T}}, \tag{63}$$

$$\boldsymbol{T} = (t_{11}, t_{12}, t_{21}, t_{22}, \cdots, t_{n_I,1}, t_{n_I,2})^{\mathrm{T}}, \tag{64}$$

$$\boldsymbol{C}^J = \begin{bmatrix} C_{11}^J & C_{12}^J \\ C_{21}^J & C_{22}^J \end{bmatrix}, \tag{65}$$

$$\boldsymbol{H}^J = \begin{bmatrix} H_{11}^{1J} & H_{12}^{1J} & H_{11}^{2J} & H_{12}^{2J} & \cdots & H_{11}^{n_I,J} & H_{12}^{n_I,J} \\ H_{21}^{1J} & H_{22}^{1J} & H_{21}^{2J} & h_{22}^{2J} & \cdots & H_{21}^{n_I,J} & H_{22}^{n_I,J} \end{bmatrix}, \tag{66}$$

$$\boldsymbol{G}^J = \begin{bmatrix} G_{11}^{1J} & G_{12}^{1J} & G_{11}^{2J} & G_{12}^{2J} & \cdots & G_{11}^{n_I,J} & G_{12}^{n_I,J} \\ G_{21}^{1J} & G_{22}^{1J} & G_{21}^{2J} & G_{22}^{2J} & \cdots & G_{21}^{n_I,J} & G_{22}^{n_I,J} \end{bmatrix}. \tag{67}$$

$$H_{ij}^{IJ} = \sum_{n=1}^{N} \int_{\Gamma_n} t_{ij}^*(\xi_J, \boldsymbol{x}) \varphi_I(\boldsymbol{x}) \mathrm{d}\Gamma, \tag{68}$$

$$G_{ij}^{IJ} = \sum_{n=1}^{N} \int_{\Gamma_n} u_{ij}^*(\xi_J, \boldsymbol{x}) \varphi_I(\boldsymbol{x}) \mathrm{d}\Gamma. \tag{69}$$

For all the nodes, we have the following linear algebraic equations

$$(\boldsymbol{C} + \boldsymbol{H}) \boldsymbol{U} = \boldsymbol{G}\boldsymbol{T}, \tag{70}$$

where

$$\boldsymbol{C}=\begin{bmatrix} \boldsymbol{C}^1 & \boldsymbol{0} & \cdots & \boldsymbol{0} \\ \boldsymbol{0} & \boldsymbol{C}^2 & \cdots & \boldsymbol{0} \\ \vdots & \vdots & \ddots & \vdots \\ \boldsymbol{0} & \boldsymbol{0} & \cdots & \boldsymbol{C}^{n_I} \end{bmatrix}, \tag{71}$$

$$\boldsymbol{H}=(\boldsymbol{H}^1, \boldsymbol{H}^2, \cdots, \boldsymbol{H}^{n_I})^{\mathrm{T}}, \tag{72}$$

$$\boldsymbol{G}=(\boldsymbol{G}^1, \boldsymbol{G}^2, \cdots, \boldsymbol{G}^{n_I})^{\mathrm{T}}. \tag{73}$$

When eq. (61) is obtained, for the nonsingular integrals in eq. (60), the standard Gaussian quadrature [27] is used; and for the singular integrals in eq. (60), the logarithmic Gaussian quadrature formula and Cauchy principle value integral [27] are used.

Substituting the boundary conditions into eq. (70) directly, and solving the equation, we obtain the displacements and tractions at nodes on the boundary Γ.

When the load point ξ is located in the domain Ω, from eq. (54) we have

$$u_i(\xi)=\sum_{n=1}^{N}\int_{\Gamma_n} u_{ki}^{*}(\xi,\boldsymbol{x})\sum_{I=1}^{n_I}\varphi_I(\boldsymbol{x})t_i(\xi_I)\mathrm{d}\Gamma - \sum_{n=1}^{N}\int_{\Gamma_n} t_{ki}^{*}(\xi,\boldsymbol{x})\sum_{I=1}^{n_I}\varphi_I(\boldsymbol{x})u_i(\xi_I)\mathrm{d}\Gamma, \tag{74}$$

and we then obtain the displacements at the point ξ. By Hook's law, the stresses at the point can then be obtained. The integrals in eq. (54) are nonsingular. The standard Gaussian quadrature [27] is used when eq. (74) is obtained.

This is the interpolating boundary element-free method (IBEFM). In the IBEFM, when the IMLS method is used, the boundary conditions can be applied directly and easily.

4 Example problems

Three example problems are selected to demonstrate the applicability of the IBEFM. The results obtained for these examples are compared with the existing analytical solutions in the literature.

The first example is Timoshenko beam problem. Consider a beam subjected to a parabolic traction at the free end as shown in Figure 1. The length of the beam is *L*, the height is *D*, and the depth is considered to be of unit. The beam is assumed to be in a state of plane stress. The analytical displacements to this problem are given by Timoshenko and Goodier [28]:

$$u_1=-\frac{px_2}{6EI}\left[(6L-3x_1)x_1+(2+\nu)\left[x_2^2-\frac{D^2}{4}\right]\right], \tag{75}$$

$$u_2=\frac{p}{6EI}\left[3\nu(L-x_1)x_2^2+(4+5\nu)\frac{D^2x_1}{4}+(3L-x_1)x_1^2\right], \tag{76}$$

where the moment of inertia I of the beam is given by

$$I=\frac{D^3}{12}. \tag{77}$$

The corresponding stresses are

$$\sigma_{11}=-\frac{p(L-x_1)x_2}{I}, \tag{78}$$

$$\sigma_{22}=0, \tag{79}$$

$$\sigma_{12}=\frac{p}{2I}\left[\frac{D^2}{4}-x_2^2\right]. \tag{80}$$

The problem is solved for the plane stress case with $E=3.0\times10^7$ Pa, $\nu=0.3$, $L=48$ m, $D=12$ m, and $p=1000$ N. The essential boundary conditions are $u_1(0,0)=u_2(0,0)=0$ and $u_1(0,6)=u_1(0,-6)=0$.

The node distribution on the boundary of the problem domain is shown in Figure 2. In our numerical implementation, the quadratic basis function is used, and the weight function is chosen as:

$$w(\boldsymbol{x}-\boldsymbol{x}_I)=\begin{cases}\dfrac{\rho^2}{|\boldsymbol{x}-\boldsymbol{x}_I|^2}\left(1-\dfrac{\rho}{|\boldsymbol{x}-\boldsymbol{x}_I|}\right)^2, & |\boldsymbol{x}-\boldsymbol{x}_I|\leqslant\rho,\\ 0, & |\boldsymbol{x}-\boldsymbol{x}_I|>\rho,\end{cases} \tag{81}$$

where ρ is the radius of the influence domain.

The numerical results by the IBEFM are presented in Figure 3 and 4. Evidently the present results are in excellent agreement with the analytical solution.

The second example is a circular ring under a distributed inner pressure. Details of the circular ring are shown in Figure 5. The distributed inner pressure $p=3.0\times10^5$, Poisson's ratio $\nu=0.25$, and the shear module $E=10^6$. The radii of the circular ring are $b=5$ and $a=1$.

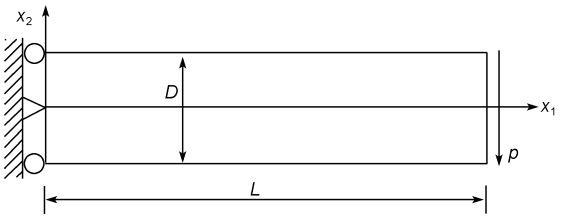

Figure 1 A cantilever beam.

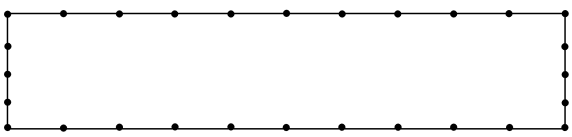

Figure 2 The nodes on the boundary of the cantilever beam.

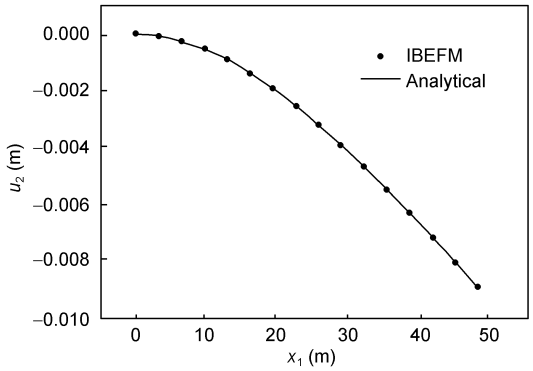

Figure 3 The displacement u_2 at x_2=0.

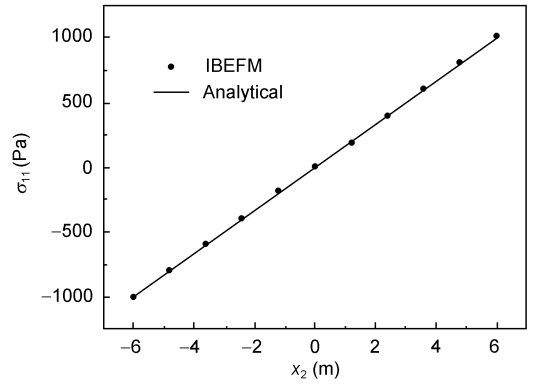

Figure 4 The stress σ_{11} at x_1=L/2.

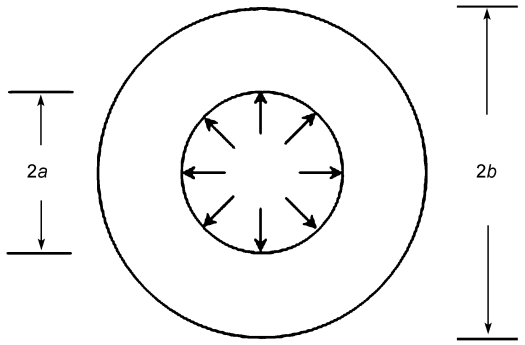

Figure 5 A circular ring under a distributed pressure.

For plane stress problems, the analytical displacement of the circular ring problem is [28]

$$u_r = \frac{a^2 pr}{E(b^2 - a^2)}\left[1 - v + \frac{b^2}{r^2}(1+v)\right], \tag{82}$$

$$u_\theta = 0. \tag{83}$$

and the corresponding stresses are

$$\sigma_r = \frac{a^2 p}{(b^2 - a^2)}\left[1 - \frac{b^2}{r^2}\right], \tag{84}$$

$$\sigma_\theta = \frac{a^2 p}{(b^2 - a^2)}\left[1 + \frac{b^2}{r^2}\right]. \tag{85}$$

Because of the symmetry of the model, only a quarter of the model needs to be considered in the analysis. Figure 6 shows the distribution of the nodes at the boundary of the domain for this problem.

To obtain a solution to this problem, we employ a total of forty nodes to model the boundary of the quarter of the model. The quadratic basis function and the weight function (81) are used. The numerical results of displacement u_r and stress σ_r at x_2=0 are presented in Figure 7 and 8. The numerical results agree well with the analytical values.

To obtain the numerical convergence of the IBEFM with respect to the number of total nodes used for discretizing the boundary of the problem domain, we employ a total of thirty-two and forty-eight nodes to model the boundary of the quarter of the model, respectively. The numerical results are shown in Figure 7 and 8 that the numerical solutions converge with the number of nodes increasing.

The third example is a perforated plate under a distributed load. As shown in Figure 9, we select a rectangular plate with a central hole. The load is p=1000 Pa. The other parameters in our analysis are Poisson's ratio v=0.25 and

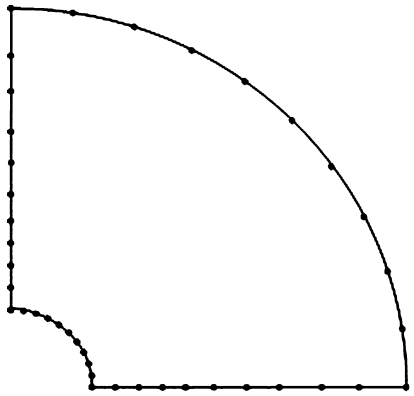

Figure 6 The nodes on the boundary of a circular ring.

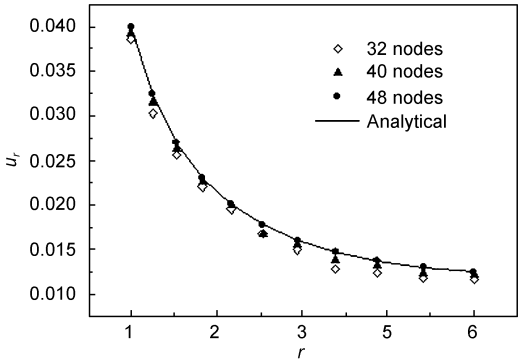

Figure 7 The displacement u_r at x_2=0.

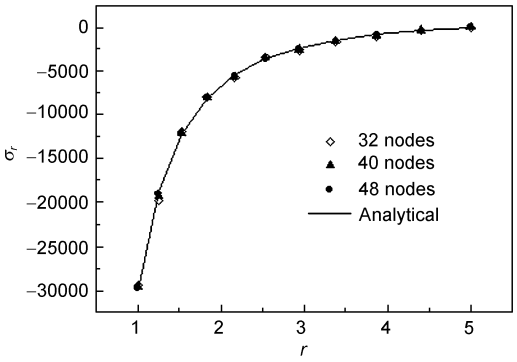

Figure 8 The stress σ_r at x_2=0.

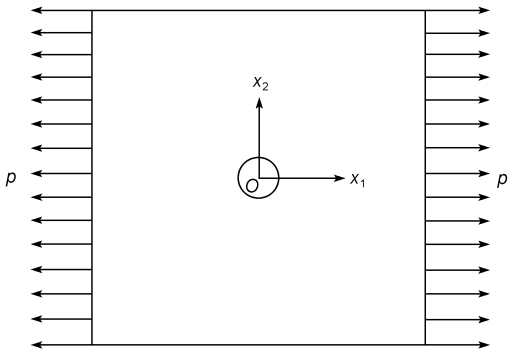

Figure 9 A rectangular plate with a hole under a distributed load.

Young's modulus E=2.0×10^5 MPa.

The analytical stresses of this perforated rectangular plate are [28]

$$\sigma_r = \frac{p}{2}\left(1-\frac{a^2}{r^2}\right)+\frac{p}{2}\cos 2\theta\left(1-\frac{a^2}{r^2}\right)\left(1-3\frac{a^2}{r^2}\right), \quad (86)$$

$$\sigma_\theta = \frac{p}{2}\left(1+\frac{a^2}{r^2}\right)-\frac{p}{2}\cos 2\theta\left(1+3\frac{a^4}{r^4}\right), \quad (87)$$

$$\tau_{r\theta} = \tau_{\theta r} = -\frac{p}{2}\sin 2\theta\left(1-\frac{a^2}{r^2}\right)\left(1+3\frac{a^2}{r^2}\right). \quad (88)$$

Because of the symmetry of the model, only a quarter of the model needs to be considered in the analysis. Figure 10 shows the distribution of the thirty-four nodes on the boundary for this problem. In our numerical implementation, the quadratic basis function and the weight function (81) are used. The stress σ_{11} at x_1=0 obtained with the IBEFM is presented in Figure 11. It is again evident that the present results are in excellent agreement with the analytical solution.

Figure 11 presents the numerical results using the IBEFM combined with the coefficients in eq. (50) obtained by Lancaster and Salkauskas [20]. The numerical results are consistent with the analytical solution and those by the IBEFM in this paper. From eqs. (40) and (50), the coefficients in the trial function obtained by Lancaster and Salkauskas [20] are more complicated than the ones in this paper. The IBEFM combined with Lancaster's function will take more CPU time than the IBEFM in this paper. The numerical results of the IBEFM in this paper are more precise than one of the results obtained using the IBEFM combined with Lancaster's function.

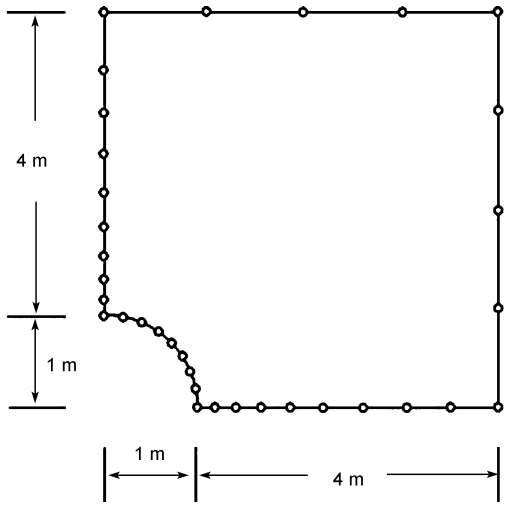

Figure 10 The nodes on the boundary of the rectangular plate with a hole.

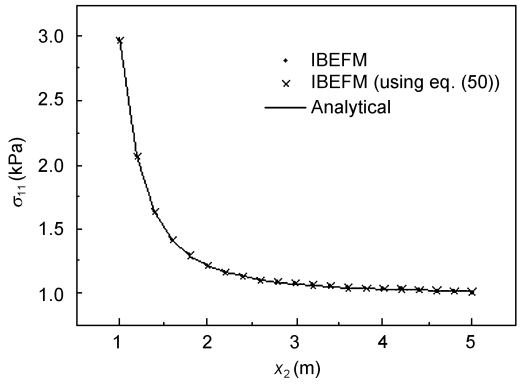

Figure 11 The stress σ_{11} at x_1=0.

5 Conclusions

This paper offers a new method to obtain the shape function of the MLS approximation and improves the interpolating moving least-squares (IMLS) method obtained by Lancaster. Based on the boundary element-free method (BEFM), and combining the boundary integral equation (BIE) method with the IMLS method, the paper presents the interpolating boundary element-free method (IBEFM) for two-dimensional elasticity problems. The IBEFM is a direct meshless boundary integral equation method in which the basic unknown quantity is the real solution to the nodal variables. In

the BEFM and the IBEFM, the essential boundary conditions are applied directly and easily. But in the IBEFM, when the IMLS method, which satisfies the property of Kronecker δ function, is used, the essential boundary conditions are naturally applied. Thus the IBEFM gives a greater computational precision. The IBEFM is a perfect direct meshless boundary integral equation method.

This work was supported by the National Natural Science Foundation of China (Grant No. 10871124), the Innovation Program of Shanghai Municipal Education Commission (Grant No. 09ZZ99), and the Shanghai Leading Academic Discipline Project (Grant No. J50103).

1 Belytschko T, Krongauz Y, Organ D, et al. Meshless method: An overview and recent developments. Comput Methods Appl Mech Eng, 1996, 139: 3–47
2 Li S F, Liu W K. Meshfree and particle methods and their applications. Appl Mech Rev, 2002, 55: 1–34
3 Mukherjee Y X, Mukherjee S. The boundary node method for potential problems. Int J Numer Methods Eng, 1997, 40: 797–815
4 Chati M K, Mukherjee S, Mukherjee Y X. The boundary node method for three-dimensional linear elasticity. Int J Numer Methods Eng, 1999, 46: 1163–1184
5 Chati M K, Mukherjee S. The boundary node method for three-dimensional problems in potential theory. Int J Numer Methods Eng, 2000, 47: 1523–1547
6 Zhu T, Zhang J, Atluri S N. A meshless numerical method based on the local boundary integral equation (LBIE) to solve linear and non-linear boundary value problems. Eng Anal Bound Elem, 1999, 23: 375–389
7 Atluri S N, Sladek J, Sladek V, et al. The local boundary integral equation (LBIE) and it's meshless implementation for linear elasticity. Comput Mech, 2000, 25: 180–198
8 Dai B D, Cheng Y M. Local boundary integral equation method based on radial basis functions for potential problems. Acta Physica Sinica, 2007, 56: 597–603
9 Cheng Y M, Peng M J. Boundary element-free method for elastodynamics. Sci China Ser G-Phys Mech Astron, 2005, 48: 641–657
10 Liew K M, Cheng Y M, Kitipornchai S. Boundary element-free method (BEFM) and its application to two-dimensional elasticity problems. Int J Numer Methods Eng, 2006, 65: 1310–1332
11 Kitipornchai S, Liew K M, Cheng Y M. A boundary element-free method (BEFM) for three-dimensional elasticity problems. Comput Mech, 2005, 36: 13–20
12 Liew K M, Cheng Y M, Kitipornchai S. Boundary element-free method (BEFM) for two-dimensional elastodynamic analysis using Laplace transform. Int J Numer Methods Eng, 2005, 64: 1610–1627
13 Cheng Y M, Liew K M, Kitipornchai S. Reply to 'Comments on 'Boundary element-free method (BEFM) and its application to two-dimensional elasticity problems''. Int J Numer Methods Eng, 2009, 78: 1258–1260
14 Sun Y Z, Zhang Z, Kitipornchai S, et al. Analyzing the interaction between collinear interfacial cracks by an efficient boundary element-free method. Int J Eng Sci, 2006, 44: 37–48
15 Liew K M, Cheng Y M, Kitipornchai S. Analyzing the 2D fracture problems via the enriched boundary element-free method. Int J Solids Struct, 2007, 44: 4220–4233
16 Liew K M, Sun Y Z, Kitipornchai S. Boundary element-free method for fracture analysis of 2-D anisotropic piezoelectric solids. Int J Numer Methods Eng, 2007, 69: 729–749
17 Qin Y X, Cheng Y M. Reproducing kernel particle boundary element-free method for elasticity. Acta Physica Sinica, 2006, 55: 3215–3222
18 Peng M J, Cheng Y M. A boundary element-free method (BEFM) for two-dimensional potential problems. Eng Anal Bound Elem, 2009, 33: 77–82
19 Liew K M, Cheng Y M. Complex variable boundary element-free method for two-dimensional elastodynamic problems. Comput Methods Appl Mech Eng, 2009, 198: 3925–3933.
20 Lancaster P, Salkauskas K. Surface generated by moving least squares methods. Math Comput, 1981, 37: 141–158
21 Zhang Z, Liew K M, Cheng Y M. Coupling of improved element-free Galerkin and boundary element methods for the 2D elasticity problems. Eng Anal Bound Elem, 2008, 32: 100–107
22 Zhang Z, Liew K M, Cheng Y M, et al. Analyzing 2D fracture problems with the improved element-free Galerkin method. Eng Anal Bound Elem, 2008, 32: 241–250
23 Zhang Z, Zhao P, Liew K M. Improved element-free Galerkin method for two-dimensional potential problems. Eng Anal Bound Elem, 2009, 33: 547–554
24 Cheng Y M, Li J H. A complex variable meshless method for fracture problems. Sci China Ser G-Phys Mech Astron, 2006, 49: 46–59
25 Liew K M, Feng C, Cheng Y M, et al. Complex variable moving least-squares method: A meshless approximation technique. Int J Numer Methods Eng, 2007, 70: 46–70
26 Peng M J, Liu P, Cheng Y M. The complex variable element-free Galerkin (CVEFG) method for two-dimensional elasticity problems. Int J Appl Mech, 2009, 1: 367–385
27 Brebbia C A, Telles J C F, Wrobel L C. Boundary Element Techniques Theory and Applications in Engineering. Berlin: Springer-Verlag, 1984
28 Timoshenko S P, Goodier J N. Theory of Elasticity. 3rd ed. New York: McGraw- Hill Inc., 1970